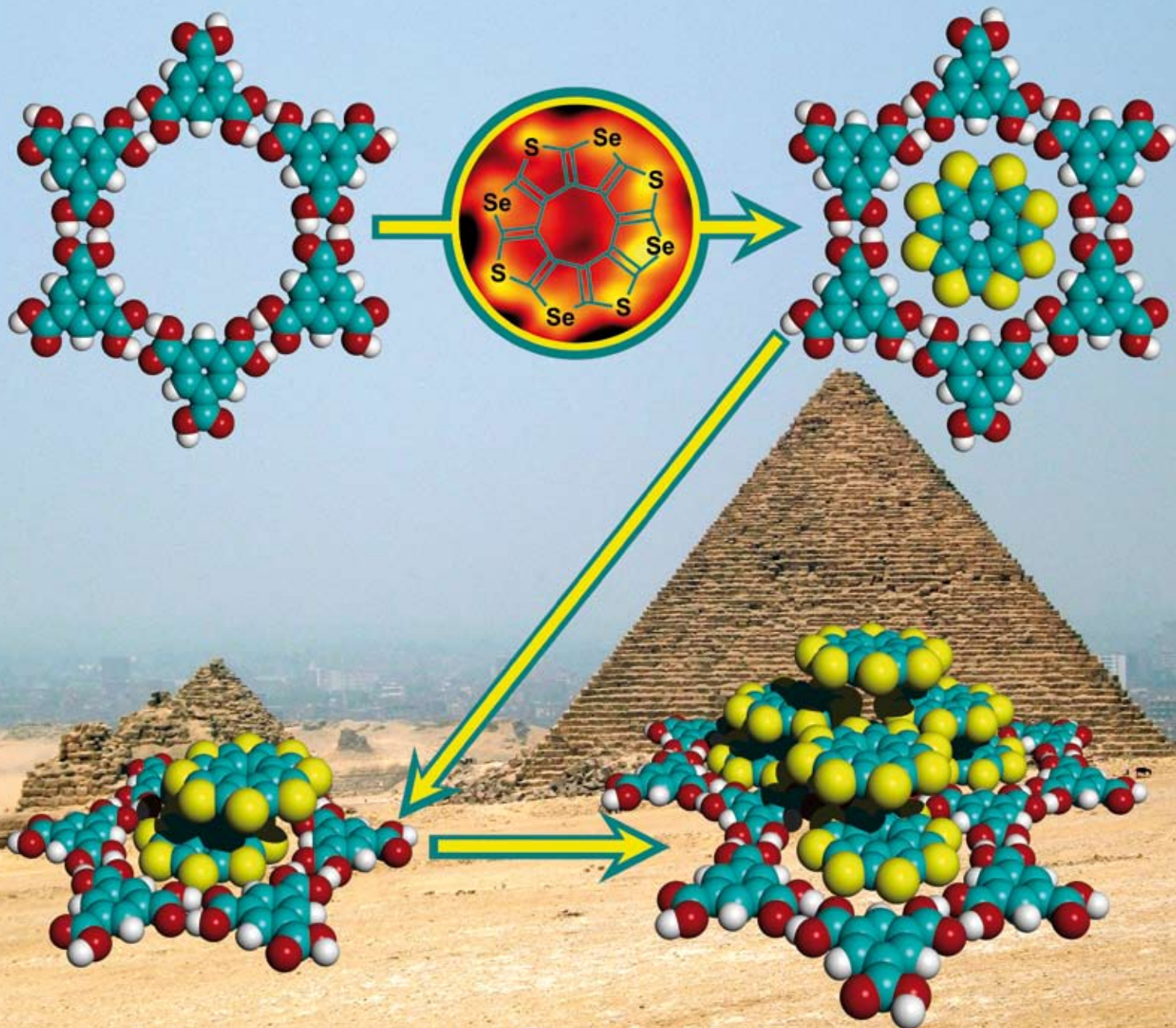


# ChemComm

Chemical Communications

www.rsc.org/chemcomm

Number 10 | 14 March 2009 | Pages 1141–1280



ISSN 1359-7345

RSC Publishing

#### COMMUNICATION

Federico Rosei,  
Dmitrii F. Perepichka *et al.*  
Supramolecular assembly of  
heterocirculenes in 2D and 3D

#### FEATURE ARTICLE

Yongfeng Zhou and Deyue Yan  
Supramolecular self-assembly of  
amphiphilic hyperbranched polymers  
at all scales and dimensions: progress,  
characteristics and perspectives

# Supramolecular assembly of heterocirculenes in 2D and 3D†

Oleksandr Ivashenko,<sup>a</sup> Jennifer M. MacLeod,<sup>b</sup> Konstantin Yu. Chernichenko,<sup>c</sup> Elizabeth S. Balenkova,<sup>c</sup> Roman V. Shpanchenko,<sup>c</sup> Valentine G. Nenajdenko,<sup>c</sup> Federico Rosei<sup>\*b</sup> and Dmitrii F. Perepichka<sup>\*a</sup>

Received (in Austin, TX, USA) 3rd November 2008, Accepted 1st December 2008

First published as an Advance Article on the web 6th January 2009

DOI: 10.1039/b819532c

The results of a high-resolution ambient STM study of ‘sulflower’ (octathio[8]circulene) and ‘selenosulfower’ (*sym*-tetraselenatetrathio[8]circulene) molecules, immobilized in a hydrogen-bonded matrix of trimesic acid (TMA) at the solid–liquid interface, are compared with the STM and X-ray structure of separate host and guest 2D and 3D crystals, respectively.

The development of scanning tunneling microscopy (STM) has enabled the direct space imaging of planar organic molecules with sub-molecular resolution.<sup>1</sup> Besides providing valuable structural information, particularly for large molecules, STM has proven to be extremely useful for studying supramolecular assembly and weak interactions between molecules adsorbed on a surface either from solution or from the gas phase.<sup>2</sup>  $\pi$ -Functional molecules are particularly interesting candidates for such studies as the charge-transport in these compounds critically depends on the supramolecular assembly.<sup>3</sup> Here we report the first STM investigation of heterocirculenes **1** and **2**, self-assembled with trimesic acid (TMA, **3**) at the solution–highly-oriented pyrolytic graphite (HOPG) interface, and show the mutual effects of the host (TMA) and guest (heterocirculenes) on each other.

Circulenes are a rare class of polyaromatic compounds built from arenes annulated into macrocycles.<sup>4</sup> Coronene, the only planar benzenoid circulene ([6]-circulene, **4**), has attracted significant attention as a guest molecule in two-dimensional molecular networks,<sup>5,6</sup> and was used itself as a building block for surface nanotemplates<sup>7</sup> and sensor fabrication.<sup>8</sup> The first fully heterocyclic circulenes, octathio[8]circulene **1**<sup>9</sup> (‘sulflower’) and its selenium analogue tetraselenotetrathio[8]circulene **2**<sup>10</sup> (‘selenosulfower’), were recently synthesized by us. **1** can also be viewed as a completely fused cyclic oligothiophene; supramolecular assembly of a non-fused cyclo[12]thiophene was studied by STM earlier.<sup>3</sup> According to X-ray crystallographic analyses, sulflower **1**<sup>9,11</sup> and selenosulfower **2** (Fig. 1) are flat, while for their smaller and larger

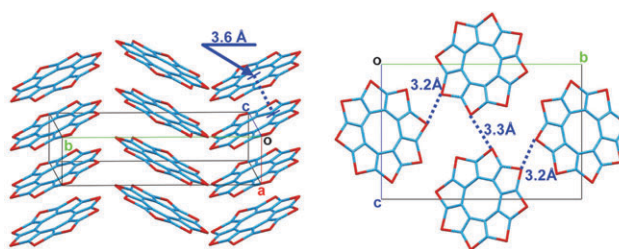
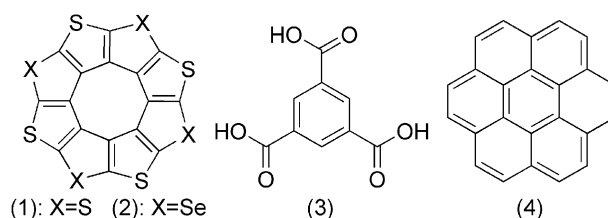


Fig. 1 Solid state packing of selenosulfower **2**, showing (left)  $\pi$ -stacked columns and (right) intercolumnar chalcogen–chalcogen contacts. Color assignment: carbon—cyan, chalcogen (S, Se)—red.

homologues (with less than 8 or more than 9 thiophene rings), bowl-shape or saddle-shape curvatures were predicted<sup>9</sup> by density functional theory (DFT) calculations. In the solid state, **1**<sup>9</sup> and **2** form tilted stacks with strong  $\pi$ – $\pi$  interactions (interplane distance 3.5–3.6 Å). Each stack (column) is surrounded by six neighboring  $\pi$ -columns, resulting in numerous chalcogen–chalcogen contacts, some of which are extremely short (3.2–3.3 Å; cf. sum of van der Waals radii (vdW) S+Se of 3.7 Å). Replacing the sulfur atom with selenium has little apparent effect on the crystal structure: both **1** and **2** pack in an identical fashion,<sup>‡</sup> although a rotational disorder is observed for selenosulfower in the columns (see ESI†).



The extensive intermolecular interaction of this packing mode makes these molecules interesting candidates for organic semiconductors. In fact, we have recently demonstrated the application of **1** and **2** in thin film transistors.<sup>10</sup> Since most of such potential applications involve the formation of supramolecular assemblies on surfaces (*e.g.* thin films, monolayers, *etc.*), it is important to know how the molecules adsorb and assemble on a surface.

While coronene can form ordered monolayers on HOPG when deposited from DMF solution,<sup>8</sup> our attempts to observe self-assembly of the heterocirculenes on HOPG using various solvents at different temperatures and conditions were unsuccessful. This might be due to the extremely low solubility<sup>9</sup> of these compounds and weaker interactions of the heterocirculenes with graphite (as compared to coronene).

<sup>a</sup> Department of Chemistry, McGill University, 801 Sherbrooke str. West, Montreal, Canada H3A 2K6.

E-mail: dmitrii.perepichka@mcgill.ca; Fax: +1 (0)514 398 3797; Tel: +1 (0)514 398 6233

<sup>b</sup> INRS Énergie, Matériaux et Télécommunications, Université du Québec, 1650 Boul. Lionel Boulet, Varennes (QC), Canada J3X 1S2. E-mail: rosei@emt.inrs.ca;

Fax: +1 (0)450 929 8102; Tel: +1 (0)450 929 8246

<sup>c</sup> Department of Chemistry, Moscow State University, 119992 Moscow, Russia

† Electronic supplementary information (ESI) available: Experimental section, crystallographic data (in cif format) for **2**; details of calculations and additional STM images. CCDC 707828. For ESI and crystallographic data in CIF or other electronic format see DOI: 10.1039/b819532c

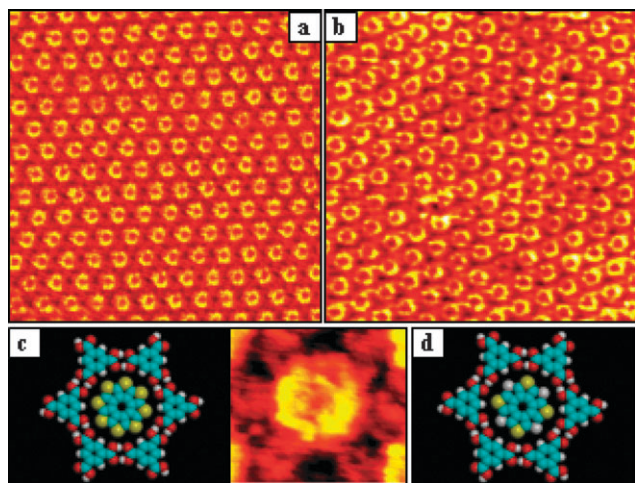


**Fig. 2** Heterocirculenes in TMA chicken-wire matrix. (a), (b) STM images with corresponding models of sulflower–TMA (c) and selenosulflower–TMA (d) SAMNs, respectively. For convenience, a  $2.0 \times 2.2$  nm zoom of the TMA–sulflower image is shown next to the model in (c). Tunneling parameters:  $I_t = 0.3$  nA,  $U_t = +0.3$  V. In models: carbon—cyan, hydrogen—white (small), oxygen—red, sulfur—yellow and selenium—white (large).

To immobilize **1** and **2** on the surface for imaging, TMA (**3**), which is known to form porous hydrogen-bonded networks, has been added to the system. At the solution–HOPG interface, TMA self-assembles in a hexagonal network.<sup>12,13</sup> The cavities formed within the polymorphs of this network have an internal vdW diameter of  $\sim 1.2$  nm and are ideal for incorporation of **1** and **2** (external vdW diameter of 1.22 nm and 1.26 nm, respectively) as guests. Applying a suspension of the corresponding heterocirculene in TMA–octanoic acid solution on HOPG results in the formation of TMA–sulflower or TMA–selenosulflower host–guest architectures (Fig. 2). The periodicity of these networks ( $1.58 \pm 0.09$  nm) matches the periodicity of the ‘parent’ TMA chicken-wire motif suggesting unperturbed structure of the host matrix and allowing for a convenient drift correction of all acquired images.

The homoassembly of TMA at the solid–liquid interface only yields one of the two stable polymorphs characterized by ‘chicken-wire’ or ‘flower’ patterns, with the latter, more densely packed polymorph being the only observed structure in short-chain fatty acid solvents (shorter than heptanoic acid).<sup>12b</sup> It is thus remarkable that in the presence of **1** or **2**, the chicken-wire (as in Fig. 1) was the only observed TMA polymorph, even when a solvent as short as propionic acid was used (see Fig. S2, ESI†). Such selective stabilization of one TMA polymorph *vs.* the other can be explained by the higher areal density of hexagonal cavities in the chicken-wire assembly (39%) as compared to the flower assembly (28%).<sup>14</sup>§ Very recently, a similar effect was demonstrated by using a coronene guest to template the formation of a 2D Kagomé network in preference to alternative close packed and parallel structures of hydrogen-bonded molecules.<sup>15</sup>

In high-resolution STM images, both sulflower **1** and selenosulflower **2** appear as circles with eight ‘petals’ (Fig. 3a and b). The  $3.3 \pm 0.3$  Å and  $9.1 \pm 0.7$  Å distances between the adjacent and opposite petals, respectively, match the

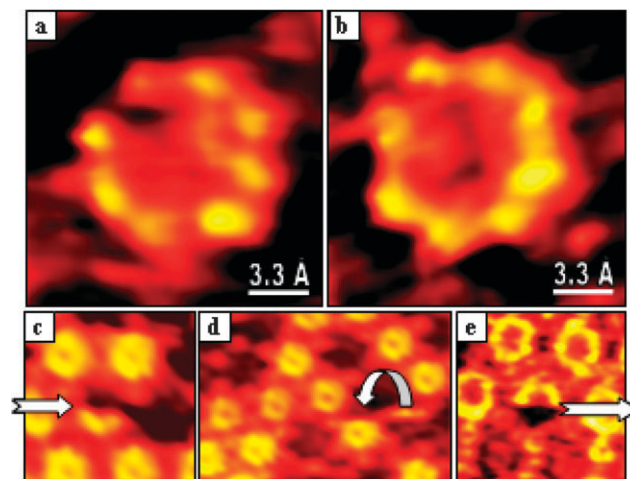


**Fig. 3** Sub-molecular resolution of the heterocirculenes ((a) sulflower–(b) selenosulflower) in TMA matrix and observation of single-molecule adsorption (c), migration (d) and desorption (e) in a partially filled TMA–sulflower SAMN (scanning direction is downwards). STM parameters: (a)  $I_t = 0.15$  nA,  $U_t = +0.5$  V; (b)  $I_t = 0.3$  nA,  $U_t = +0.6$  V; (c)  $4.2 \times 4.2$  nm,  $I_t = 0.3$  nA,  $U_t = +0.3$  V; (d)  $8.1 \times 5.4$  nm,  $I_t = 0.3$  nA,  $U_t = +0.3$  V; (e)  $4.2 \times 4.2$  nm,  $I_t = 0.3$  nA,  $U_t = +0.3$  V. For convenience, white arrows indicate guest molecules that exhibit dynamic phenomena.

corresponding chalcogen–chalcogen distances in these heterocirculenes (**1**:  $d_{S1-S2} = 3.25$  Å,  $d_{S1-S5} = 8.49$  Å; **2**:  $d_{S1-Se2} = 3.31$  Å,  $d_{S1-S5} = 8.52$  Å and  $d_{Se2-Se6} = 8.78$  Å).¶ Resolution of these ‘petals’ together with an analysis of average spacing for adjacent petals along fast and slow scan directions indicates that any rotation of the heterocirculenes within the TMA cavities is much slower than the timescale of STM imaging (0.1 s per line). DFT calculated closest host–guest contacts are 3.17 Å (S···O, for **1**···**3**) and 3.16 Å (Se···O, for **2**···**3**), which are shorter than the sums of vdW radii (3.32 Å and 3.42 Å, respectively) explaining the tight rotational fixation of these heterocirculenes by the host matrix. For all-benzenoid circulene **4** incorporated into the same TMA host matrix, the observed partial site-specific fixation of the guest molecules was explained by the strong influence of the underlying HOPG.<sup>6</sup> In the case of **1** and **2**, the only manifestation of the substrate influence was an occasionally observed very weak moiré pattern (ESI†).

The adsorption dynamics of the heterocirculenes **1** and **2** are slower than formation of the TMA network and thus it is often possible to observe gradual filling of the host cavities. Imaging partially filled networks allowed us to observe single-molecule adsorption–desorption phenomena. The ‘incomplete’ appearance of the sulflower as a semicircle is associated with adsorption (Fig. 2c), migration (Fig. 2d) and desorption (Fig. 2e) of the molecule during the scan. Although these processes occur spontaneously at room temperature, they can be additionally influenced by the STM tip<sup>6</sup> which may even be used to induce total desorption of the TMA–heterocirculene SAMN in the scanned area (see Fig. S4, ESI†). Local perturbation by the scanning tip might also be a reason for the observed smearing of the heterocirculene petals in the high-resolution images (see ESI†).

The increase of the concentration of sulflower and TMA upon gradual drying of the solution leads to an accumulation

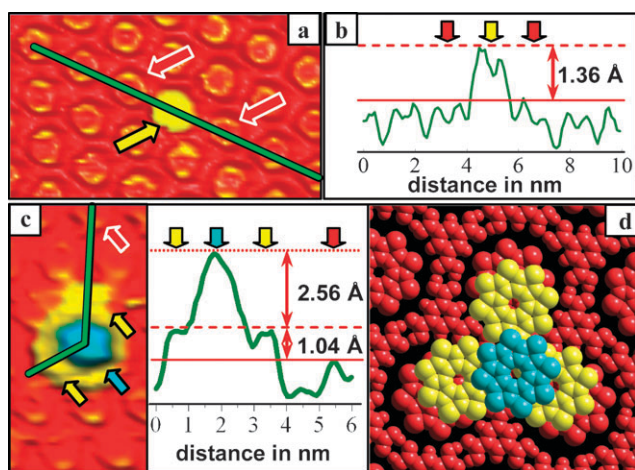


**Fig. 4** Interactions in the heterocirculene–TMA systems: (a) an STM image of sulflower dimer with the corresponding line profile (b); (c) sulflower island with its line profile (inset) and a tentative structural model shown in (d). Arrows assignment: red—normal sulflower inclusions, yellow—sulflower dimers, blue—the pick of the sulflower island. STM parameters: (a)  $6 \times 10$  nm,  $I_t = 0.13$  nA,  $U_t = +1.2$  V; (c)  $4.1 \times 8.0$  nm,  $I_t = 0.13$  nA,  $U_t = +1.2$  V.

of multilayers on the surface. The first step of this process is shown in Fig. 4a. The line profile (Fig. 4b) shows a feature with the lateral dimensions of a sulflower guest, but approximately double the normal height, suggesting the formation of a  $\pi$ – $\pi$  sulflower dimer. Similar structures were also observed for coronene multilayers on Au(111).<sup>16</sup> The coronene dimers, however, are believed to be unstable at the solid–liquid interface,<sup>6</sup> so the observation of their sulflower analogue highlights the role of sulfur–sulfur interactions as a driving force for molecular self-assembly. Moreover it was possible to observe larger agglomerates as shown in Fig. 4c. These can be described as three-layer structures in which three adjacent sulflower dimers form a base for further out-of-plane growth of sulflower “wires” (Fig. 4d). The height profile suggests the possible accumulation of two molecules (or out-of-plane adsorption) in the third layer, but this cannot be positively established since the height profile in STM images incorporates both topography and electronic information. Similar structures were also formed in the selenosulflower–TMA system (see ESI†) thus illustrating the strong preference of **1** and **2** towards self-aggregation.

To conclude, the immobilization of heterocirculene molecules within a rigid H-bonded matrix allowed their STM investigation on HOPG at the liquid–solid interface, and revealed that:

(i) heterocirculene guests stabilize preferentially the chicken-wire TMA polymorph, which has the highest areal density of adsorption sites;

(ii) the high local density of states at chalcogen atoms make them the highest contrast parts of the molecules, that can easily be resolved with ambient STM at the solvent–HOPG interface;

(iii) the combination of  $\pi$ – $\pi$  and chalcogen–chalcogen interactions favors the self-aggregation of these heterocirculenes into dimers and larger structures with the possibility to form multilayers of host–guest architectures featuring 1D

heterocirculene stacks—an interesting material morphology for electronic device applications.

We acknowledge financial support from NSERC (Discovery Grants to F.R. and D.F.P.), Centre for Self-Assembled Chemical Structures, AirForce Office of Scientific Research, DuPont (Young Professor Award to D.F.P.) and the Canada Research Chairs program (partial salary support to F.R.).

## Notes and references

† Crystal data for **2**: colorless needles,  $C_{16}S_4Se_{3.317}$ , FW = 604.2, monoclinic,  $P2_1/m$  [14],  $a = 4.0290(8)$  Å,  $b = 16.680(3)$  Å,  $c = 11.270(2)$  Å,  $\beta = 94.30(3)^\circ$ ,  $V = 755.3(2)$  Å<sup>3</sup>,  $Z = 2$ , No. of measured/independent reflection ( $I \geq 2\sigma$ ): 2731/1032,  $R_{eq} = 0.033$ ,  $R = 0.064$ ,  $R_{all} (I > 2\sigma(I)) = 0.078$ , GOF = 1.35. **2** was rotationally disordered in the crystal between S and Se positions (see ESI†). Crystal data for **1** were reported elsewhere (ref. 9).

§ The value for the flower pattern in the original paper (ref. 14) (16%) was calculated for the period  $a = 2.5$  nm. We instead refer here to the UHV studies by the same authors (ref. 12a) as well as DFT calculations which suggest  $a = 2.7$  nm, in which case the density of cavities for this polymorph is 28%.

¶ As calculated at DFT-B3LYP/6-31G(d) level.

- 1 F. Rosei, M. Schunack, P. Jiang, A. Gourdon, E. Laegsgaard, I. Stensgaard, C. Joachim and F. Besenbacher, *Prog. Surf. Sci.*, 2003, **71**, 95.
- 2 (a) S. De Feyter and F. C. De Schryver, *Chem. Soc. Rev.*, 2003, **32**, 139; (b) F. Cicoira, C. Santato and F. Rosei, *Top. Curr. Chem.*, 2008, **285**, 203.
- 3 E. Mena-Osteritz and P. Bauerle, *Adv. Mater.*, 2006, **18**, 447.
- 4 (a) R. Scholl and K. Meyer, *Ber. Dtsch. Chem. Ges.*, 1932, **65**, 902; (b) J. H. Dopfer and H. Wynberg, *J. Org. Chem.*, 1975, **40**, 1957, and ref. therein.
- 5 (a) S. Furukawa, K. Tahara, F. C. De Schryver, M. Van der Auweraer, Y. Tobe and S. De Feyter, *Angew. Chem., Int. Ed.*, 2007, **46**, 2831; (b) D. Wu, K. Deng, M. He, Q. Zeng and C. Wang, *ChemPhysChem*, 2007, **8**, 1519; (c) J.-R. Gong, H.-J. Yan, Q.-H. Yuan, L.-P. Xu, Z.-S. Bo and L.-J. Wan, *J. Am. Chem. Soc.*, 2006, **128**, 12384; (d) J. Lu, S.-B. Lei, Q.-D. Zeng, S.-Z. Kang, C. Wang, L.-J. Wan and C.-L. Bai, *J. Phys. Chem. B*, 2004, **108**, 5161.
- 6 S. J. H. Griessl, M. Lackinger, F. Jamitzky, T. Market, M. Hietschold and W. M. Heckl, *Langmuir*, 2004, **20**, 9403.
- 7 S. Yoshimoto, E. Tsutsumi, R. Narita, Y. Murata, M. Murata, K. Fujiwara, K. Komatsu, O. Ito and K. Itaya, *J. Am. Chem. Soc.*, 2007, **129**, 4366.
- 8 H.-X. Zhang, Q. Chen, R. Wen, J.-S. Hu and L.-J. Wan, *Anal. Chem.*, 2007, **79**, 2179.
- 9 K. Yu. Chernichenko, V. V. Sumerin, R. V. Shpanchenko, E. S. Balenkova and V. G. Nenajdenko, *Angew. Chem., Int. Ed.*, 2006, **45**, 7367.
- 10 A. Davdov, F. Cicoira, K. Yu. Chernichenko, E. S. Balenkova, R. M. Osuna, F. Rosei, V. G. Nenajdenko and D. F. Perepichka, *Chem. Commun.*, 2008, 5354.
- 11 T. Fujimoto, R. Suizu, H. Yoshikawa and K. Awaga, *Chem.–Eur. J.*, 2008, **14**, 6053.
- 12 (a) S. Griessl, M. Lackinger, M. Edelwirth, M. Hietschold and W. M. Heckl, *Single Mol.*, 2002, **3**, 25; (b) M. Lackinger, S. Griessl, W. M. Heckl, M. Hietschold and G. W. Flynn, *Langmuir*, 2005, **21**, 4984.
- 13 (a) K. G. Nath, O. Ivasenko, J. M. MacLeod, J. A. Miwa, J. D. Wuest, A. Nanci, D. F. Perepichka and F. Rosei, *J. Phys. Chem. C*, 2007, **111**, 16996; (b) J. M. MacLeod, O. Ivasenko, D. F. Perepichka and F. Rosei, *Nanotechnology*, 2007, **18**, 424301.
- 14 L. Kampschulte, M. Lackinger, A.-K. Maier, R. S. K. Kishore, S. Griessl, M. Schmittel and W. M. Heckl, *J. Phys. Chem. B*, 2006, **110**, 10829.
- 15 M. Blunt, X. Lin, M.-C. Gimenez-Lopez, M. Schröder, N. R. Champness and P. H. Beton, *Chem. Commun.*, 2008, 2304.
- 16 S. Uemura, M. Sakata, I. Taniguchi, C. Hirayama and M. Kunitake, *Thin Solid Films*, 2002, **409**, 206.